

FT-IR Spectroscopic Imaging of Anisotropic Poly(3-hydroxybutyrate)/Poly(lactic acid) Blends with Polarized Radiation

Christian Vogel,[†] Elke Wessel,[‡] and Heinz W. Siesler^{*,†}

Department of Physical Chemistry, University of Duisburg-Essen, Schuetzenbahn 70, D-45117 Essen, Germany, and Research and Development, Beiersdorf AG, Unnastrasse 48, D-20253 Hamburg, Germany

Received January 21, 2008

Revised Manuscript Received March 27, 2008

Introduction. Biodegradable polymers¹ are a group of polymers which can be produced from renewable resources by bacteria and have the fundamental advantage of being biodegradable. In this communication uniaxially elongated films of different blends of poly(3-hydroxybutyrate) and poly(lactic acid) were analyzed by FT-IR spectroscopic imaging. Poly(3-hydroxybutyrate) (PHB)² is the most common member of the poly(hydroxyalkonates) (PHAs), which has the disadvantage of being stiff and brittle because of its high crystallinity. In contrast, the poly(lactic acid) (PLA)³ used here contains 10% of *meso*-lactic acid, and as a consequence it has only a crystallinity of ~32% (see below) and is flexible.

Blends of PHB and PLA have been analyzed with different techniques by several research groups.^{4–7} Recently, FT-IR imaging results on the phase behavior of PHB/PLA blends with different compositions have been published.⁸ The present communication reports FT-IR imaging data obtained with polarized radiation on different PHB/PLA blends which had been previously investigated by rheo-optical FT-IR spectroscopy and subjected to uniaxial mechanical elongation.

FT-IR spectroscopic imaging^{9,10} offers the possibility to combine spectral and spatial information, thereby enabling a chemical visualization of samples. Thus, sample areas of $3.9 \times 3.9 \text{ mm}^2$ or $260 \times 260 \text{ }\mu\text{m}^2$ can be analyzed by FT-IR transmission spectroscopy without or in combination with a microscope, respectively, with a lateral resolution up to 10–15 μm . First reports on the use of polarized radiation for the production of FT-IR images have been reported by Wilhelm et al.¹¹ and Koenig et al.¹²

Rheo-optical FT-IR measurements combine a stress–strain test with in-situ polarization measurements to detect the structural information on a molecular level simultaneously to the mechanical treatment. For the detailed experimental and theoretical principles of rheo-optical FT-IR/FT-NIR spectroscopy, the reader is referred to the relevant literature.^{13–15}

In previous investigations of the mechanical elongation of PLA-rich ($\geq 60 \text{ wt } \%$ PLA) PHB/PLA blend films (35 °C, 10% strain per minute) interesting orientation phenomena of the PHB and PLA chains have been detected. Thus, in these blends the PLA chains orient in the direction of elongation whereas the PHB chains orient perpendicular to the drawing direction. This has been attributed to a continuum mechanical alignment of the long axes of the lamellar PHB domains which are embedded in the PLA matrix (see below).¹⁶ PHB/PLA blend films with

PHB > PLA compositions, on the other hand, exhibit similar mechanical properties to PHB homopolymer and could only be oriented by cold drawing in ice–water after quenching from the melt.¹⁷ In these films the polymer chains of both PHB and PLA exhibited a preferential chain alignment parallel to the drawing direction.

Experimental Section. Materials. Bacterially synthesized poly(3-hydroxybutyrate) (Sigma-Aldrich, $M_w = 437\,000 \text{ g/mol}$) and poly(lactic acid) (Natureworks LLC, Minnetonka, MN) were used for the experiments without further purification. The PLA used for our experiments had a low crystallinity and was flexible because it contained 10% *meso*-lactic acid ($M_w = 240\,000 \text{ g/mol}$, $M_w/M_n = 1.8$; crystallinity by DSC = 32% ($\Delta H_{(100\% \text{ cryst PLA})} = 93 \text{ J/g}$)¹⁸).

For the preparation of PHB/PLA blend films (50/50 and 40/60 wt %) the homopolymers were dissolved in chloroform p.A in the corresponding ratios and films were prepared by casting from these solutions on roughened microscope slides (to avoid interference fringes in the transmission spectra) and subsequent evaporation of the chloroform at 35 °C in vacuum for 2 h. Films with a thickness of 27 μm (PHB/PLA 50/50 wt %) and 48 μm (PHB/PLA 40/60 wt %) were peeled off the glass slides, and stripes were cut with a length of 20 mm and a width of 6 mm. These specimens were then mounted with an initial length of 8 mm between the clamps of the stretching machine (see below) and elongated to 50% and 200% strain, respectively, at 35 °C.

Instrumentation. The PHB/PLA blends were uniaxially elongated in a miniaturized stretching machine with an elongation rate of 10% strain per minute. This machine is controlled by a Visual C++ program running under Windows 2000.¹⁹

FT-IR imaging measurements of the stretched polymer blend films in the relaxed state were taken using a Bruker imaging system (Bruker Optik GmbH, Ettlingen, Germany), which consists of an IFS66/S FT-IR spectrometer, an infrared microscope (Hyperion 3000) coupled with a macroimaging chamber (IMAC), and a 64×64 (4096) mercury cadmium telluride (MCT) focal plane array (FPA) detector (Santa Barbara Focalplane, Goleta, CA). The size of the FPA detector is $3.9 \times 3.9 \text{ mm}^2$ with the size of one detector pixel $61 \times 61 \text{ }\mu\text{m}^2$. Each image was measured in transmission for sample areas of $260 \times 260 \text{ }\mu\text{m}^2$ (with the $15\times$ objective) and $3.9 \times 3.9 \text{ mm}^2$ (in the macrochamber), with a spectral resolution of 8 cm^{-1} , and 10 scans were coadded per spectrum. Imaging spectra were recorded from the identical area with radiation polarized parallel and perpendicular, respectively, to the strain direction of the film samples. The spectra and images were evaluated using the Bruker software OPUS 5.0.

To monitor the changes in chain orientation as a consequence of the mechanical treatment, the $\nu(\text{C=O})$ absorption bands of the PHB/PLA blend films were evaluated to calculate the orientation function f_{\perp} (assuming a perpendicular transition moment of the $\nu(\text{C=O})$ absorption bands relative to the polymer chain direction) by

$$f_{\perp} = -2 \frac{R - 1}{R + 2} \quad (1)$$

where $R = A_{\parallel}/A_{\perp}$ is the dichroic ratio of the $\nu(\text{C=O})$ absorption bands in the polarization spectra. The $\nu(\text{C=O})$ bands were evaluated with a baseline from 1880 to 1600 cm^{-1} , and the peak areas under the left wing from 1825 to 1779 cm^{-1} and under the right wing from 1718 to 1691 cm^{-1} were assumed to be characteristic for the PLA and PHB components, respectively. To monitor changes in the state of order as a function of the mechanical treatment, the structural absorbance A_0 , which eliminates the effect of orientation on band intensities, has been used:

$$A_0 = \frac{A_{\parallel} + 2A_{\perp}}{3} \quad (2)$$

Results and Discussion. The measurement of the PHB/PLA (50/50 wt %) blend film was performed on a $3.9 \times 3.9 \text{ mm}^2$

* To whom correspondence should be addressed: e-mail: hw.siesler@unidue.de.

[†] University of Duisburg-Essen.

[‡] Beiersdorf AG.

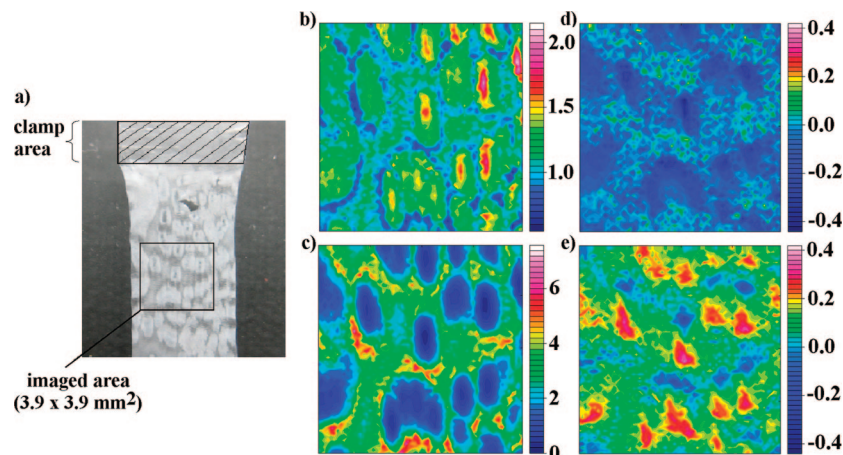


Figure 1. Optical image (a) and FT-IR images ($3.9 \times 3.9 \text{ mm}^2$) of $A_{0\text{PHB}}/A_{0\text{PLA}}$ (b) and $A_{0\text{PLA}}/A_{0\text{PHB}}$ (c) and the corresponding orientation function (f_{\perp}) images of PHB (d) and PLA (e) of the 50% stretched PHB/PLA (50/50 wt %) blend film (for optimum comparison the f_{\perp} images (d) and (e) are shown with the same color scale).

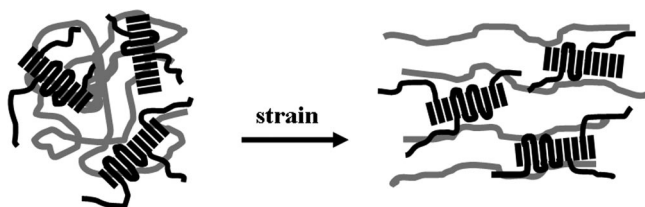


Figure 2. Schematic representation of the orientation mechanism in the PHB-rich domains of a phase-separated PHB/PLA (50/50 wt %) blend film (black: PHB chains; gray: PLA chains).

area because during elongation white areas with a length of up to about $800 \mu\text{m}$ (“islands”) (Figure 1a) developed, and a representative FT-IR image had to be expanded over a larger area. Because of sample thickness inhomogeneities in the stretched polymer film (the “islands” had a thickness of $\sim 5 \mu\text{m}$ and the matrix $\sim 18 \mu\text{m}$), the structural absorbance ratios $A_{0\text{PHB}}/A_{0\text{PLA}}$ and $A_{0\text{PLA}}/A_{0\text{PHB}}$, which compensate for these thickness differences, are presented in Figures 1b,c. Figures 1b,c indicate that the “islands” are PHB-rich and the matrix has a higher PLA content. From the orientation function (f_{\perp}) images of the corresponding sample area a negative orientation ($f_{\perp} \approx -0.4$) can be derived for the PHB chains in the “islands” (Figure 1d), whereas the PLA orients positively in the same domains ($f_{\perp} \approx 0.3$) (Figure 1e). In the matrix, on the other hand, both PHB and PLA orient only very slightly positive (f_{\perp} between 0 and 0.1) (Figures 1d,e). Thus, the two phases of the unstretched PHB/PLA (50/50 wt %) blend film with uniform thickness respond differently to the applied mechanical stress: the PHB-rich phase is extended to higher degrees and lower thickness with opposite orientation of the two polymer components (PHB negative, PLA positive), whereas the PLA-rich phase undergoes only a small elongation with negligible thickness reduction and very low positive orientation for both polymer components. The orientation mechanism of the PHB-rich phase with opposite alignment of the PHB (negative) and PLA (positive) chains is also commonly observed in the hard segments of polyurethanes.¹⁴ It can be explained on the basis of a continuum mechanical alignment of the long axes of PHB lamellae embedded in PLA chains with comparatively low structural order (Figure 2).

Figure 3a shows the FT-IR polarization spectra of the $3.9 \times 3.9 \text{ mm}^2$ area discussed above, however, measured with a single-element detector. Thus, a perpendicular dichroism (corresponding to a preferential orientation of the polymer chains in the

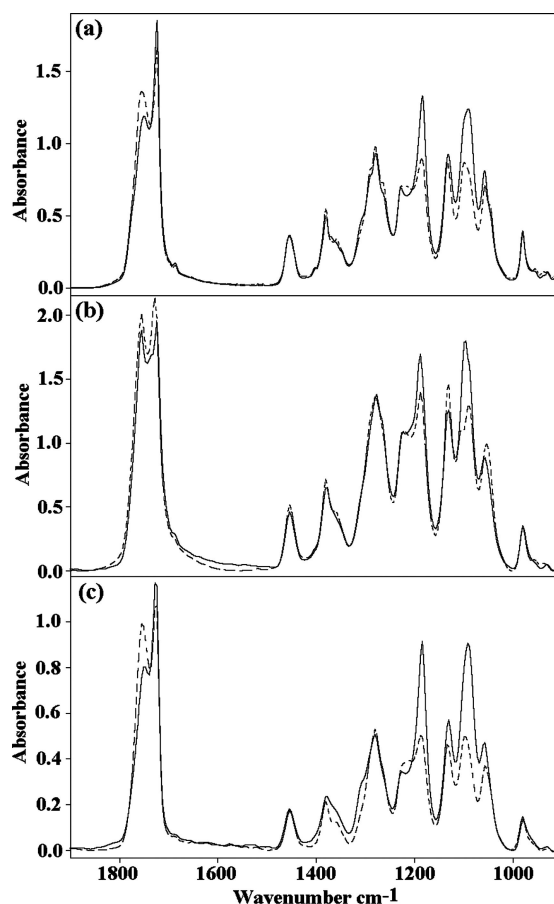


Figure 3. FT-IR polarization spectra ((—) parallel and (---) perpendicular to the strain direction) measured with a single-element detector of the whole area (A) and with one pixel in the matrix area (B) and “island” area (C) of the 50% elongated PHB/PLA (50/50 wt %) blend film.

drawing direction) is observed for the $\nu(\text{C}=\text{O})$ absorption of PLA and a parallel dichroism (corresponding to a preferential perpendicular chain orientation) for the $\nu(\text{C}=\text{O})$ absorption of the PHB component. Parts b and c of Figure 3 show the FT-IR imaging polarization spectra of pixels located in the matrix and in an “island”, respectively. In accordance with the discussion of Figures 1d,e they reflect a slightly positive orientation for PHB and PLA in the matrix and an opposite orientation for the two polymer components (PHB negative, PLA positive) in the

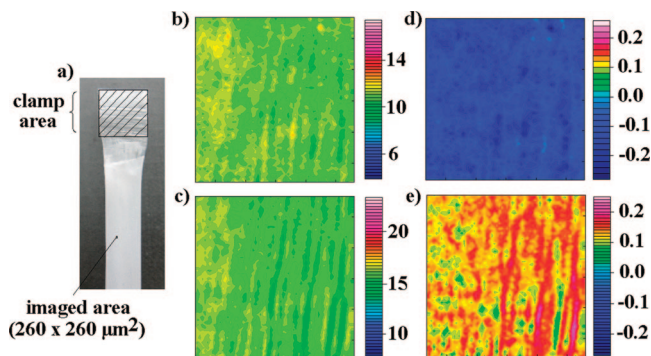


Figure 4. Optical image (a) and FT-IR images ($260 \times 260 \mu\text{m}^2$) of A_{OPHB} (b) and A_{OPLA} (c) and the corresponding orientation function (f_L) images of PHB (d) and PLA (e) of the 200% stretched PHB/PLA (40/60 wt %) blend film (for optimum comparison the f_L images (d) and (e) are shown with the same color scale).

“islands”. These figures clearly demonstrate that the polarization spectra recorded with a single-element detector cannot discriminate the different orientation mechanisms in the phase-separated, anisotropic structure of this polymer blend.

Figure 4a shows the optical image of a 200% stretched PHB/PLA (40/60 wt %) blend film. In previous investigations⁸ PHB/PLA blend films with PLA contents >50 wt % were classified as miscible because in their DSC diagrams only one T_g was detected. Here, too, the elongated polymer appears homogeneous with a uniform thickness and is slightly white colored. A preliminary $3.9 \times 3.9 \text{ mm}^2$ FT-IR imaging measurement (not shown here) showed a very homogeneous distribution of PHB and PLA over the imaged area. Thus, for the detection of microscopic structural changes a $260 \times 260 \mu\text{m}^2$ area was imaged of this anisotropic blend film. The images of A_{OPHB} and A_{OPLA} are displayed in Figures 4b,c. These images show slightly streaky patterns with reference to the distribution of PHB and PLA over the sampled area. Figure 4d displays the orientation function (f_L) image of PHB. Over the whole area a negative orientation function f_L in the range -0.05 to -0.25 was found. In contrast, the orientation function f_L of PLA (Figure 4e) is positive over the whole image (0.05 – 0.25). In this image, the observed streak pattern resembles the PLA content image (Figure 4c) with the lower PLA orientation function values in the PLA-rich areas. Nevertheless, an opposite orientation of the two polymer components (PHB negative, PLA positive) was detected over the whole image area.

Conclusions. FT-IR images measured with polarized radiation allowed to differentiate the orientation mechanisms of incompatible and miscible PHB/PLA blends, respectively, upon uniaxial elongation. Thus, in phase-separated PHB/PLA (50/50 wt %) blend films the PHB-rich domains are elongated to much higher degrees and correspondingly to much lower sample thickness than the surrounding PLA-rich matrix. In these PHB-rich areas the PHB chains show a large negative orientation ($f_L \approx -0.4$), whereas the PLA chains are oriented preferentially parallel to the drawing direction ($f_L \approx +0.3$). In contrast, the

elongated PLA-rich matrix is characterized by a low positive orientation ($f_L \approx +0.1$) for both blend components. From polarization spectra recorded of the same area with a single-element detector the different orientation mechanisms in the phase separated domains could not be discriminated. Instead, an opposite alignment of the PHB (negative) and PLA (positive) chains was simulated over the whole area. For the elongated film of the miscible PHB/PLA (40/60 wt %) blend a slight streak pattern in the elongation direction was obtained in the composition as well as orientation related images. In the orientation function (f_L) images an opposite orientation (PHB negative, PLA positive) was detected over the whole image area. With reference to the streak pattern for the PLA orientation function image a lower positive chain alignment could be detected for the PLA-richer areas. Thus, the application of the FT-IR imaging technique with polarized radiation provides far superior details in terms of the characterization of orientation phenomena in anisotropic materials compared to imaging data with unpolarized radiation as well as to dichroic measurements with a single-element detector.

Acknowledgment. The authors thank the Dr. Jost-Henkel-Stiftung (Düsseldorf, Germany) for the financial support of Christian Vogel and Prof. Y. Ozaki and his research group for the supply of polymer samples and helpful discussions.

References and Notes

- Gross, R. A.; Klara, B. *Science* **2002**, *297*, 803.
- Hocking, P. J.; Marchessault, R. H. *Polyhydroxyalkanoates. In Biopolymers from Renewable Resources*; Kaplan, D. L., Ed.; Springer-Verlag: Berlin, 1998; p 220.
- Auras, R.; Harte, B.; Selke, S. *Macromol. Biosci.* **2004**, *4*, 835.
- Blümm, E.; Owen, A. J. *Polymer* **1995**, *36*, 4077.
- Furukawa, T.; Sato, H.; Murakami, R.; Zhang, J.; Duan, Y.-X.; Noda, I.; Ochiai, S.; Ozaki, Y. *Macromolecules* **2005**, *38*, 6445.
- Ohkoshi, I.; Abe, H.; Doi, Y. *Polymer* **2000**, *41*, 5985.
- Park, J. W.; Doi, Y.; Iwata, T. *Biomacromolecules* **2004**, *5*, 1557.
- Vogel, C.; Wessel, E.; Siesler, H. W. *Biomacromolecules* **2008**, *9*, 523.
- Bhargava, R.; Wang, S.-Q.; Koenig, J. L. *Adv. Polym. Sci.* **2003**, *163*, 137.
- Bhargava, R.; Levin, I. W., Eds.; *Spectrochemical Analysis Using Infrared Multichannel Detectors*; Blackwell Publ. Ltd.: Oxford, UK, 2005.
- Chernev, B.; Wilhelm, P. *Monatsh. Chem.* **2006**, *137*, 963.
- Snively, C. M.; Koenig, J. L. *J. Polym. Sci., Part B: Polym. Phys.* **1999**, *37*, 2353.
- Siesler, H. W.; Holland-Moritz, K. *Infrared and Raman Spectroscopy*; Marcel Dekker: New York, 1980.
- Siesler, H. W.; Hoffmann, G. G.; Kolomiets, O.; Pfeifer, F.; Zahedi, M. *Variable-Temperature Rheo-Optical Fourier Transform Infrared Spectroscopy of Polymers. In Vibrational Spectroscopy of Polymers: Principles and Practice*; Everall, N. J., Chalmers, J. M., Griffiths, P. R., Eds.; John Wiley & Sons Ltd.: Chichester, UK, 2007; p 313.
- Dechant, J. *Ultrarotspektroskopische Untersuchungen an Polymeren*; Akademie-Verlag: Leipzig, 1972.
- Vogel, C. PhD Thesis, University of Duisburg-Essen, Essen, Germany, 2008.
- Iwata, T. *Macromol. Biosci.* **2005**, *5*, 689.
- Fischer, E. W.; Sterzel, H. J.; Wegner, G. *Kolloid Z. Z. Polym.* **1973**, *251*, 980.
- Hoffmann, G. G., unpublished.

MA800139U